

Institute of High Energy Physics
Chinese Academy of Sciences

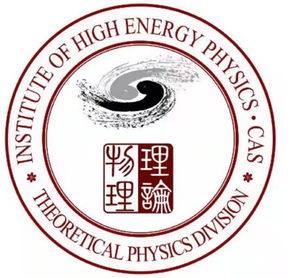

Pulsar Polarization Arrays

Jing Ren (任婧)

IHEP, CAS

The 12th KIAS Workshop on Particle Physics and Cosmology
and 2024 Korea-France STAR workshop
November 20th, 2024

Based on works with Tao Liu and others, arXiv: 2111.10615, 2304.04735, PPTA work

Content

- Pulsar timing arrays (PTAs) and pulsar polarization arrays (PPAs)
- Ultralight axion-like dark matter (ALDM) as target of PPAs
- First PPA Limits on ultralight ALDM with PPTA DR3
- Summary and outlook

Pulsars

- Pulsars emit electromagnetic pulses with extra-ordinary regularity
- Till now ~3000 pulsars observed in our galaxy
- Millisecond pulsars (MSPs) are especially stable and play roles as *astronomical clocks*

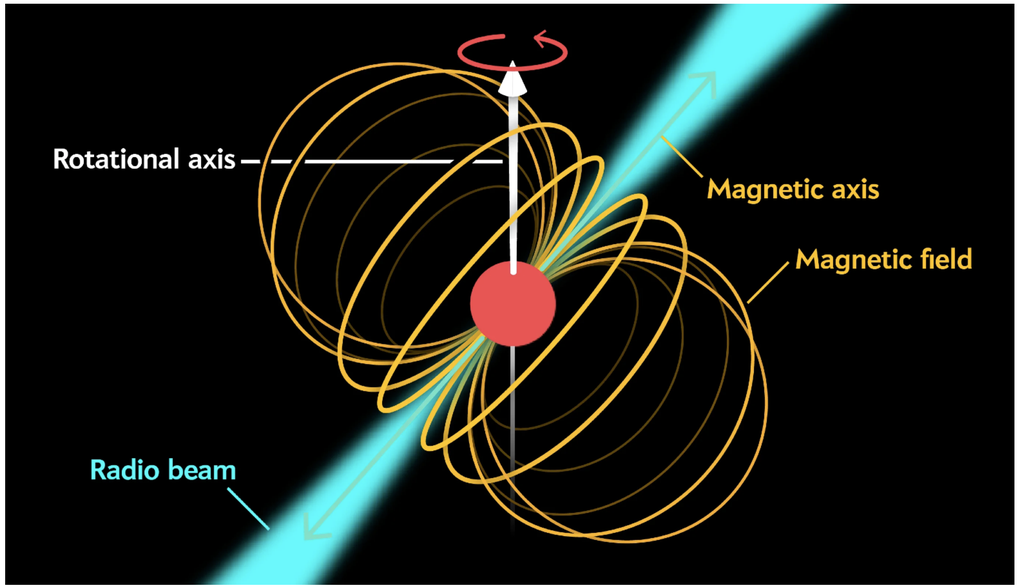

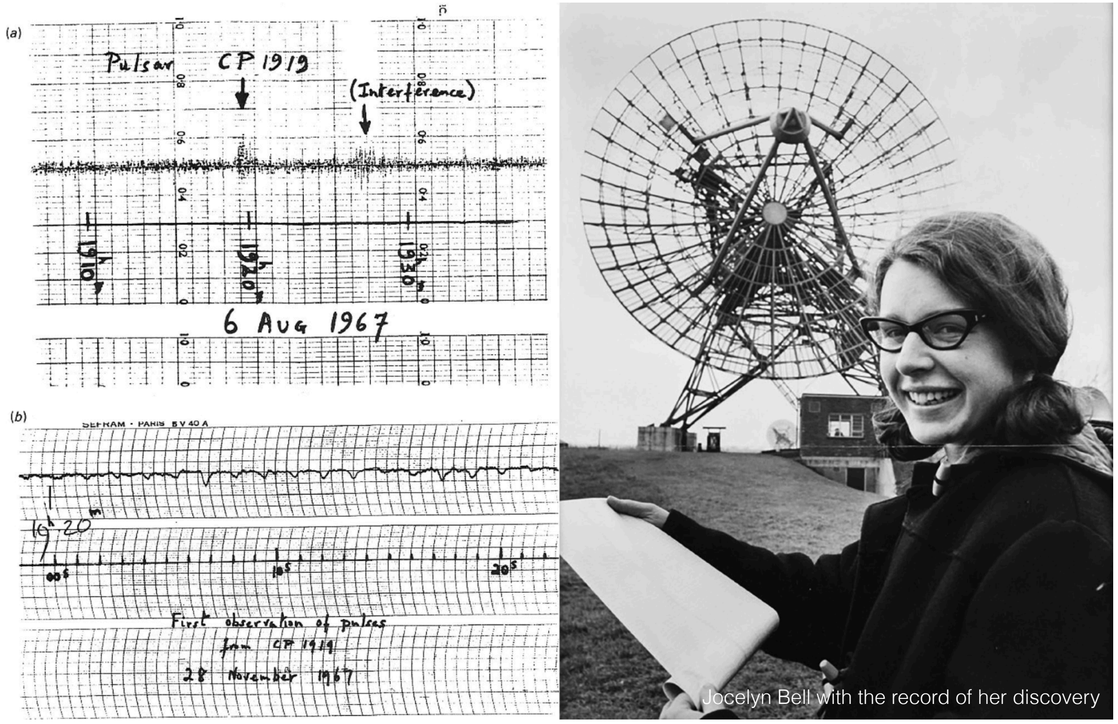

Jocelyn Bell with the record of her discovery

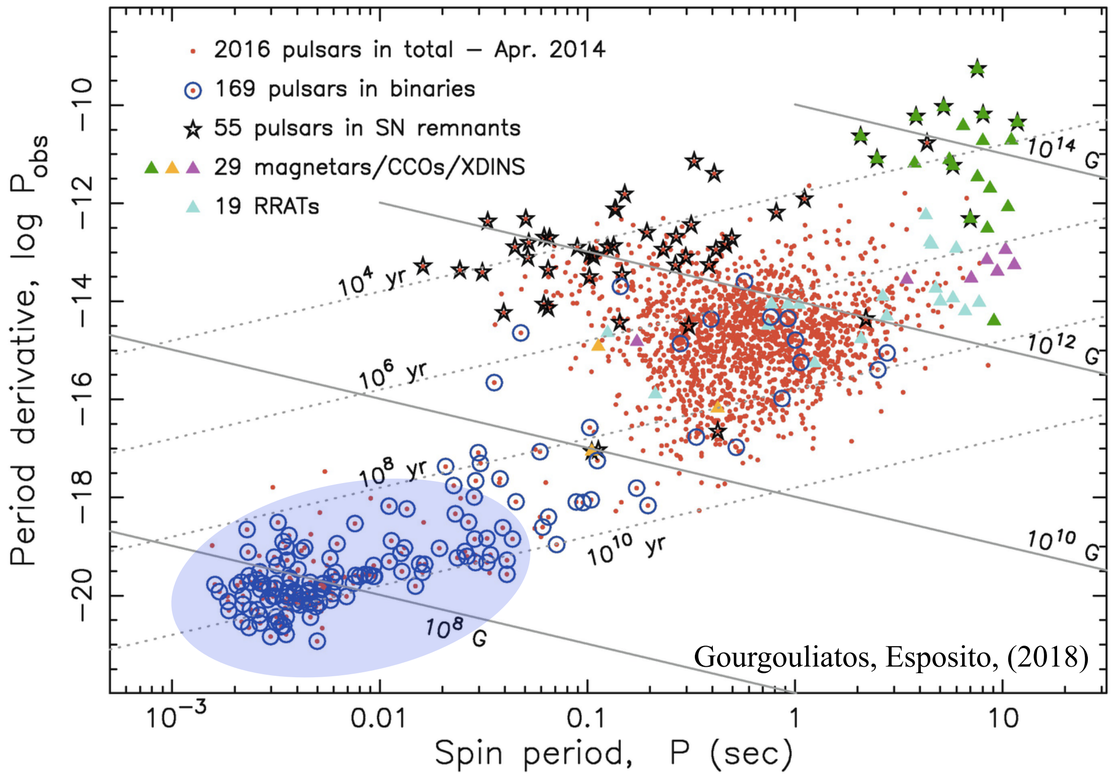

Pulsar timing arrays (PTAs)

- Given precise timing model of the expected time of arrival of the pulse, the measured **time difference** can be directly related to **gravitational waves (GWs)**

$$\Delta T(t) = \int_{-\infty}^{\infty} df \frac{1}{2} u^a u^b h_{ab}(f,\hat{n})\, e^{i2\pi f(t+\hat{n}\cdot\vec{r}_2/c)} \frac{1}{i2\pi f} \frac{1}{1+\hat{n}\cdot\hat{u}} \left[1 - e^{-\frac{i2\pi f L}{c}(1+\hat{n}\cdot\hat{u})}\right]$$

metric perturbation — "Earth" — "pulsar"

- PTAs with MSPs in different directions serve as **galactic-scale GW detectors**

- Global PTA network monitors over 80 MSPs for 10+ years. FAST/SKA may increase number to O(100)

- Stochastic GW backgrounds (SGWBs) can be identified by the **quadrupolar spatial correlations among pulsars (Hellings-Downs curve)**

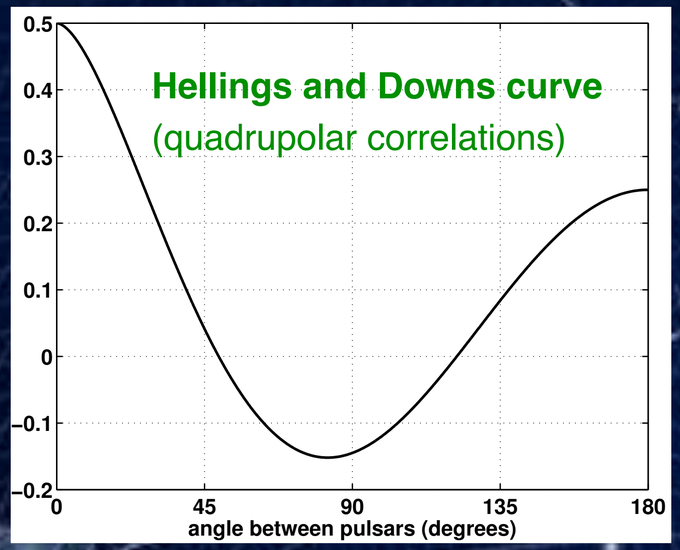

[Hellings and Downs, ApJL 265 (1983)]

Key evidence for nHz SGWBs

Compelling evidence for a *HD-correlated*, common-spectrum red noise

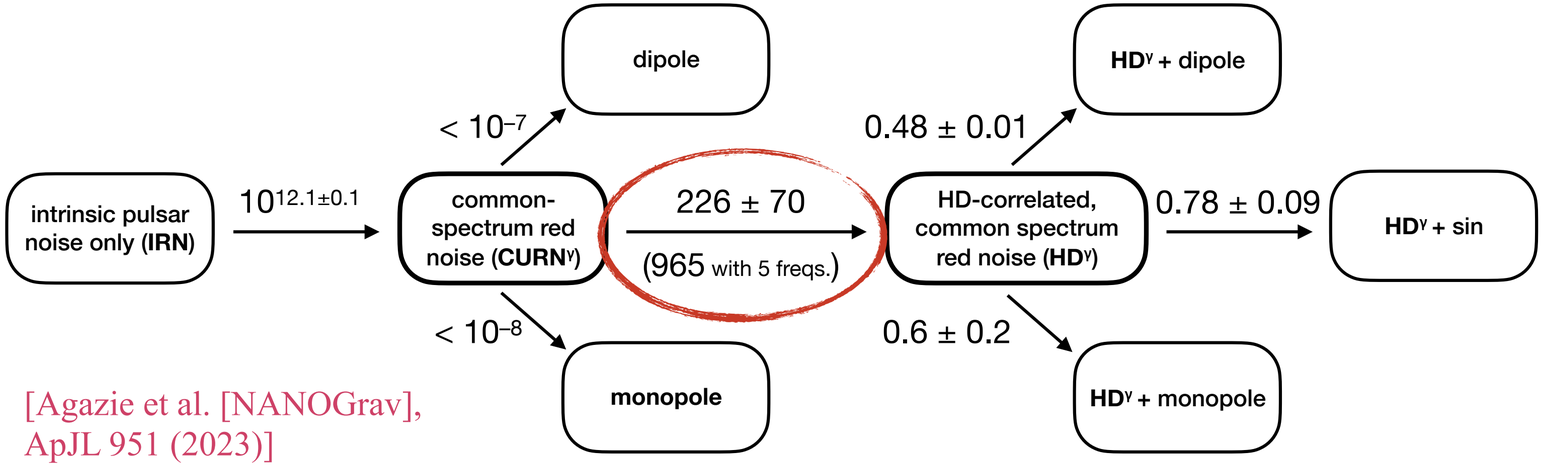

[Agazie et al. [NANOGrav], ApJL 951 (2023)]

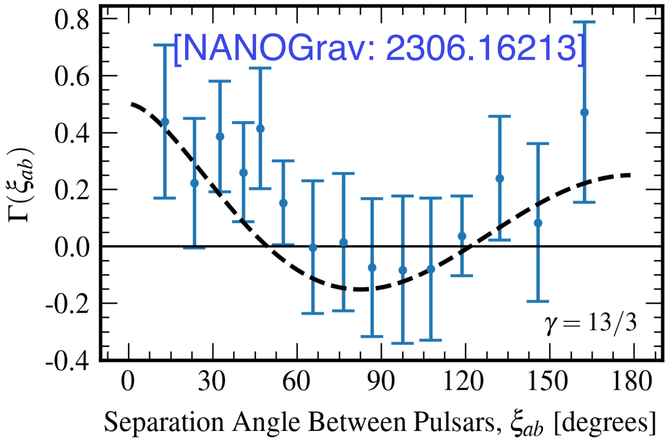

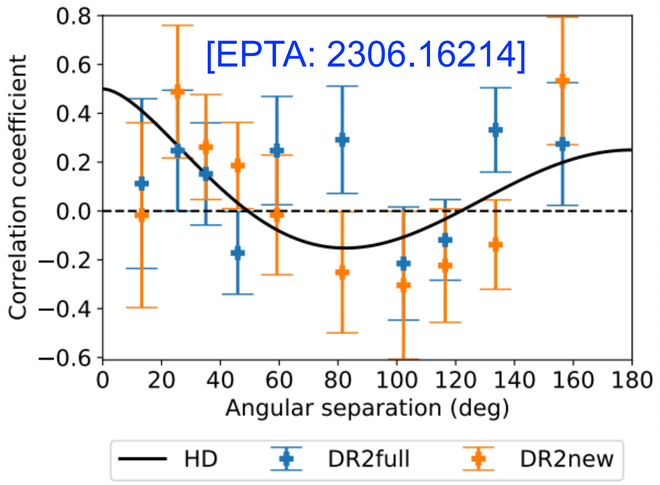

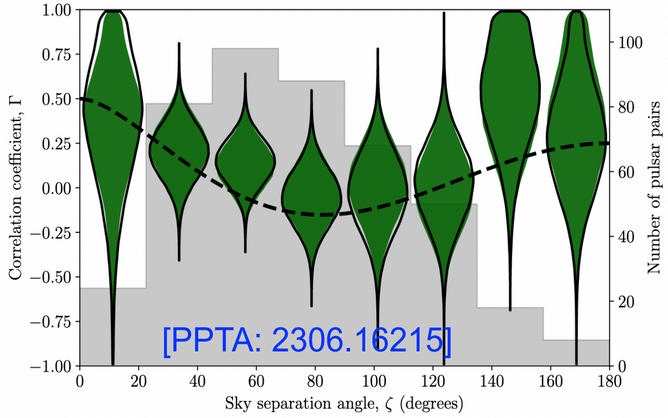

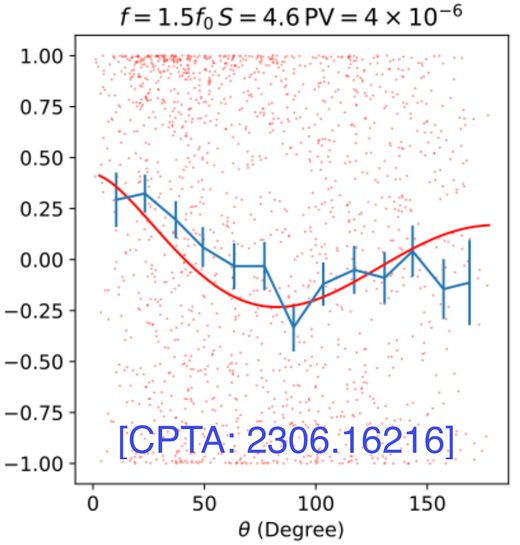

Pulsars as linear polarizers

- Pulsar radio emissions typically have strong linear polarization
- Polarization profiles are usually obtained as a *by-product of PTAs* for the purpose of calibration

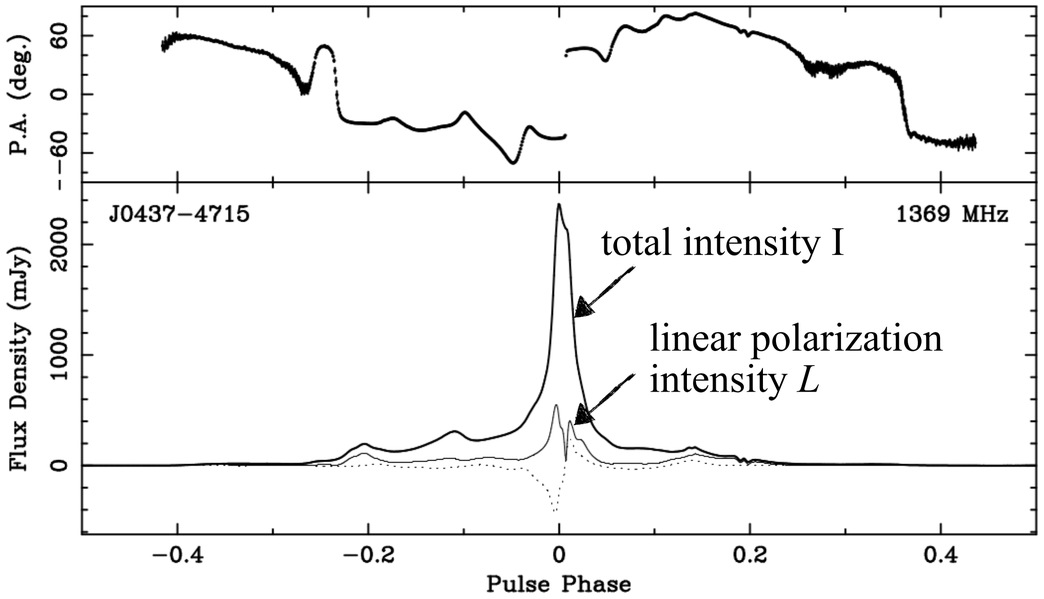

[Yan et al. (PPTA collaboration), MNRAS (2011)]

Stokes parameters: $\{I, U, Q, V\}$

Polarization angle (PA): $\mathrm{PA} = \frac{1}{2}\arctan\left(\frac{U}{Q}\right)$

Time series of PA residuals (average over phase bin)

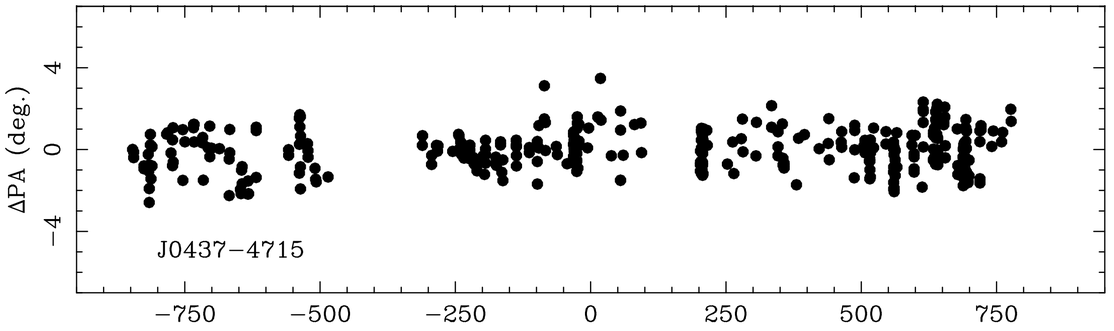

[Yan et al. (PPTA collaboration), ASS (2011)]

PHYSICAL REVIEW LETTERS

Highlights Recent Accepted Collections Authors Referees Search Press

Pulsar Polarization Arrays

Tao Liu, Xuzixiang Lou, and Jing Ren
Phys. Rev. Lett. **130**, 121401 – Published 23 March 2023

Article References No Citing Articles Supplemental Material PDF HTML

ABSTRACT

Pulsar timing arrays (PTAs) consisting of widely distributed and well-timed millisecond pulsars can serve as a galactic interferometer to measure gravitational waves. With the same data acquired for PTAs, we propose to develop pulsar polarization arrays (PPAs), to explore astrophysics and fundamental physics. As in the case of PTAs, PPAs are best suited to reveal temporal and spatial correlations at large scales that are hard to mimic by local noise. To demonstrate the physical potential of PPAs, we consider detection of ultralight axionlike dark matter (ALDM), through cosmic birefringence induced by its Chern-Simons coupling. Because of its tiny mass, the ultralight ALDM can be generated as a Bose-Einstein condensate, characterized by a strong wave nature. Incorporating both temporal and spatial correlations of the signal, we show that PPAs have a potential to probe the Chern-Simons coupling up to $\sim 10^{-14} - 10^{-17}\,\mathrm{GeV}^{-1}$, with a mass range $\sim 10^{-27}$–$10^{-21}\,\mathrm{eV}$.

Measured polarization angle

$$\mathrm{PA} = \mathrm{PA}_{\mathrm{source}} + \mathrm{PA}_{\mathrm{instru}} + \mathrm{PA}_{\mathrm{propa}}$$

- **Source**: change of pulsar orientation/ magnetosphere; stochastic variation of single pulse profile (jitter noise)
- **Instrument**: related to PA calibration; radiometer noise
- **Propagation**: Faraday rotation caused by interstellar magnetic field/Earth's ionosphere

Cross-correlate PA data to fully strengthen its capability to explore astrophysics and fundamental physics, as a precision astronomical tool

A variety of theoretical candidates of DM

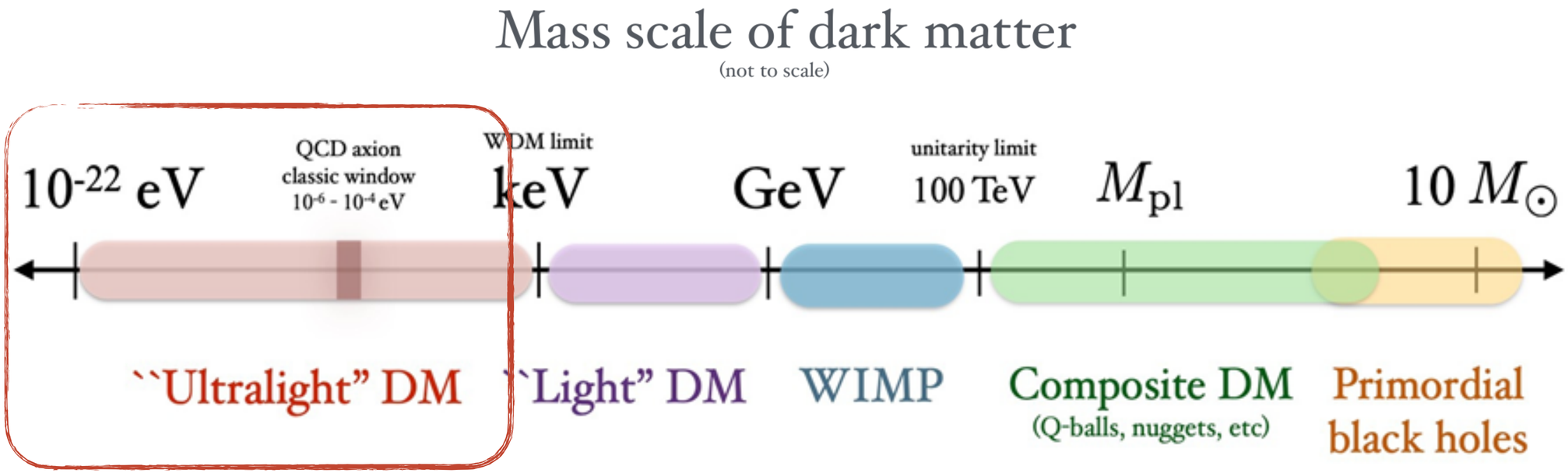

- Different types of candidates: distinct characteristics + different detection methods
- **Ultralight DM:** wavelike + Pulsar Timing/Polarization Arrays

$$N_{\rm dB} = \rho_{\rm DM}\lambda_{\rm dB}^3 \sim \left(\frac{34{\rm eV}}{m_a}\right)^4\left(\frac{250{\rm km}/s}{v}\right)^3$$

occupation number per de Broglie volume >>1 when m_a≪30eV

Ultralight dark matter (ULDM)

- Axion-like particles (ALPs): light and interact feebly, e.g. QCD axion, string axions
- For $m_a \ll 30$eV, nonthermal wave dark matter can be generated as a Bose-Einstein condensate through misalignment mechanism
- Fuzzy DM ($m_a \sim 10^{-22}$eV) address small-scale problems

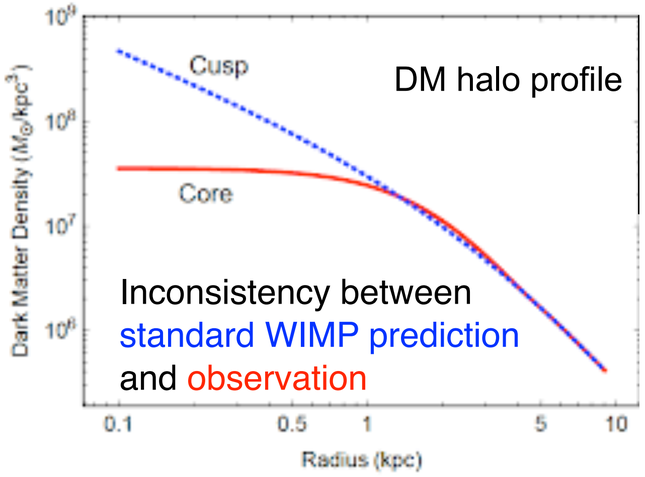

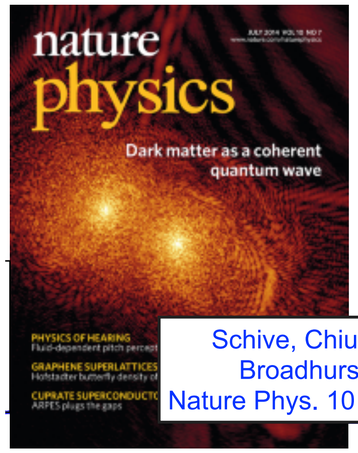

Schive, Chiueh, Broadhurst
Nature Phys. 10 (2014)

Due to condensation, a dense soliton core forms at galactic center, with a radius ~ de-Broglie wavelength ~ O(100) pc

ALPs landscapes

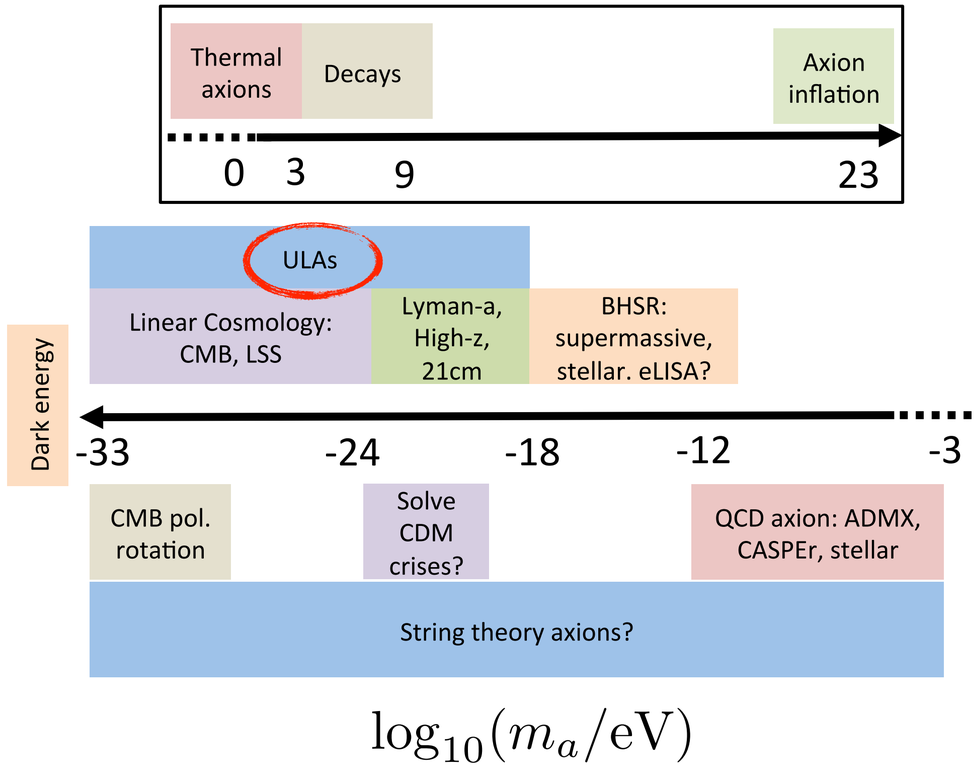

$\log_{10}(m_a/\mathrm{eV})$

[D. Marsh, Phys. Rept. 643 (2016)]

Recent constraints on ULDM, i.e. Lyman-α, dwarf galaxies, may suffer from uncertainties — different searches needed!

Physical properties of ULDM

- Local ULDM field viewed as a random superposition of a large number of plane waves

  [Foster, Rodd, Safdi, PRD 97 (2018)]

energy density

velocity distribution peaked at $v_0 \sim 10^{-3}c$

$$a(\mathbf{x},t) = \frac{\sqrt{\rho(\mathbf{x})}}{m_a} \sum_d \alpha_d \sqrt{f_{\mathbf{x}}(\mathbf{v}_d)(\Delta v)^3} \cos[\omega_a(t - \mathbf{v}_d \cdot \mathbf{x}) + \phi_d]$$

random amplitude (Rayleigh)

non-relativistic $\omega_a \approx m_a$

random phase (uniform)

- ALPs effective action: gravitational interaction, coupling to SM particles…

$$S = \int d^4x\sqrt{-g}\left[\frac{1}{2}\nabla^\mu a \nabla_\mu a - \frac{1}{2}m_a^2 a^2 + \frac{g_{a\gamma}}{2} a F_{\mu\nu}\tilde{F}^{\mu\nu} + \frac{g_{af}}{2m_f}\nabla_\mu a(\bar{f}\gamma^\mu\gamma_5 f) + ...\right]$$

gravitational coupling — Chern-Simons coupling

PTA limits on ULDM induced timing signal

- Ultralight scalar DM: $\phi(\mathbf{x},t) = A(\mathbf{x})\cos\left(m\,t + \alpha(\mathbf{x})\right)$
- ULDM induces temporal oscillating gravitational potential through stress tensor; changes the arrival frequency and time of arrival for pulses [Khmelnitsky and Rubakov, JCAP 02 (2014)]

$$\Psi(\mathbf{x},t) \simeq \Psi_0(\mathbf{x}) + \Psi_c(\mathbf{x})\cos(2mt + 2\alpha(\mathbf{x}))$$

$$f = \frac{2m}{2\pi} = 4.8\times10^{-8}\left(\frac{m}{10^{-22}\mathrm{eV}}\right)\mathrm{Hz}$$

$$\Psi_c(\mathbf{x}) = \pi\frac{G\rho_{DM}(\mathbf{x})}{m^2} \approx 6.1\times10^{-18}\left(\frac{m}{10^{-22}\,\mathrm{eV}}\right)^{-2}\left(\frac{\rho_{\mathrm{SF}}}{0.4\,\mathrm{GeV\,cm^{-3}}}\right)$$

$$\Delta t(t) = \frac{\Psi_c(x_e)}{2\pi f}\sin[2\pi f t + 2\alpha(x_e)] - \frac{\Psi_c(x_p)}{2\pi f}\sin\left[2\pi f\left(t - \frac{d_p}{c}\right) + 2\alpha(x_p)\right]$$

"Earth" **"Pulsar"**

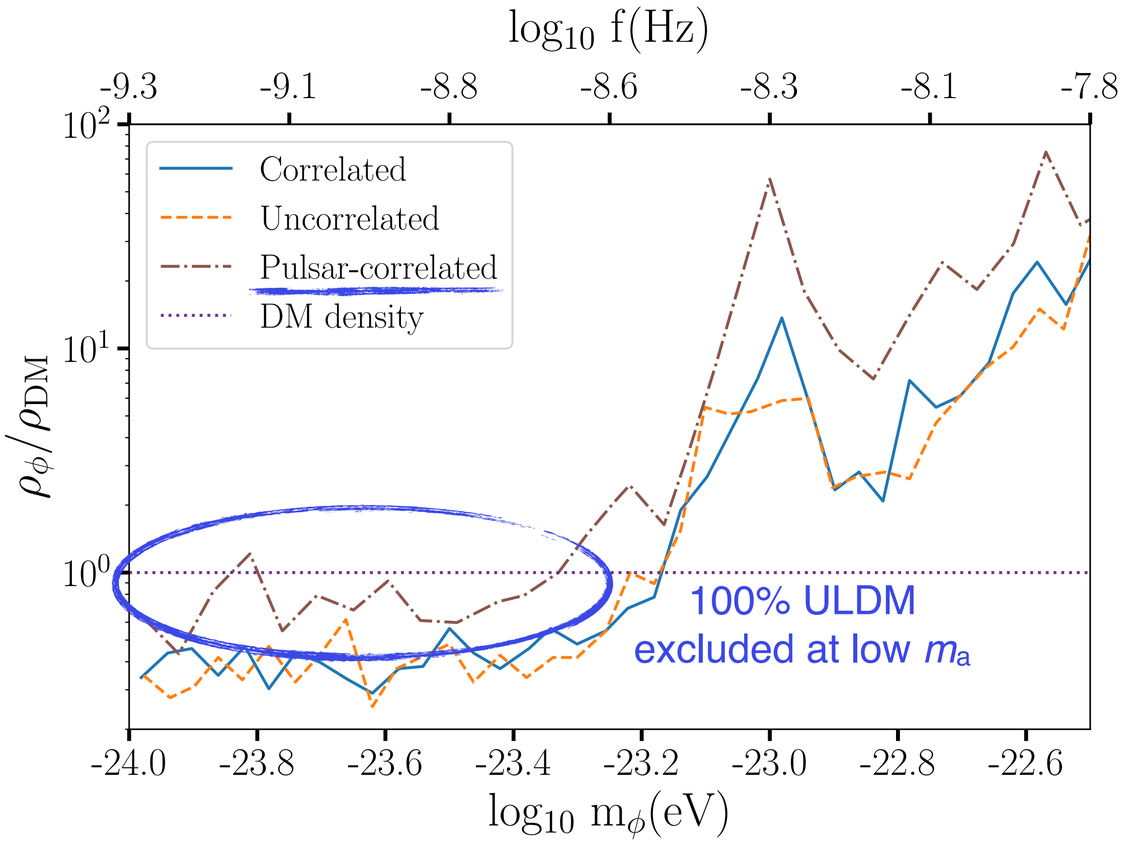

The ULDM-induced correction can be > 20 ns for m < 10^{-23} eV

[Smarra *et al.* [EPTA], PRL 131 (2023)]

ALDM induced cosmic birefringence

Chern-Simons coupling corrects the dispersion relations of two circular polarization modes of photons, yielding position angle (PA) rotation of linearly polarized photons

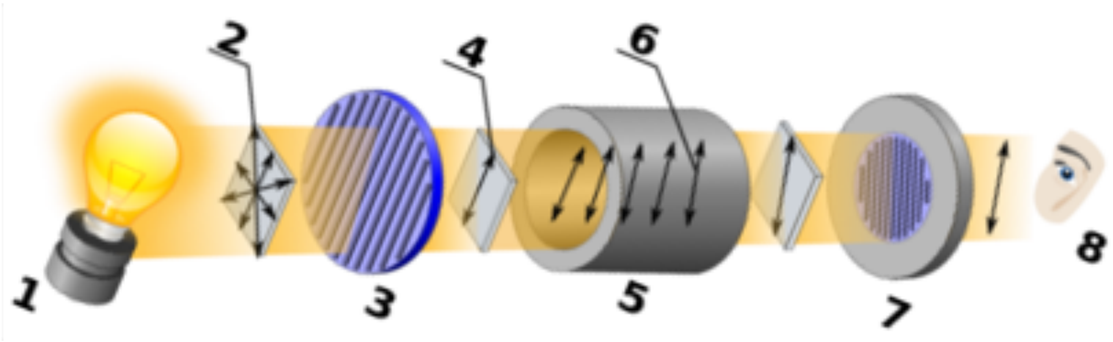

$$\omega_\pm \simeq k \pm g_{a\gamma\gamma}\left(\frac{\partial a}{\partial t} + \nabla a \cdot \frac{\mathbf{k}}{k}\right) = k \pm g_{a\gamma\gamma} n^\mu \nabla_\mu a$$

$$\Delta \mathrm{PA}^a \simeq -g_{a\gamma\gamma}\int_C ds\, n^\mu \nabla_\mu a(\mathbf{x},t) \approx g_{a\gamma\gamma}[a(\mathbf{x}_p,t_p) - a(\mathbf{x}_e,t_e)]$$

(C: the photon traveling path, n^μ: the null tangent vector to C)

"Pulsar" **"Earth"**

Compared to Faraday Rotation (FR):

- relies only on field profiles at two endpoints of photon traveling
- quasi-monochromatic oscillation around the frequency $\omega_a \approx m_a$
- no frequency dependence (increases with wavelength)

Detection of cosmic birefringence

A variety of **astrophysical and cosmological light sources** proposed to detect cosmic birefringence

PHYSICAL REVIEW D VOLUME 43, NUMBER 12 15 JUNE 1991

ARTICLES

Einstein equivalence principle and the polarization of radio galaxies

Sean M. Carroll and George B. Field
Harvard-Smithsonian Center for Astrophysics, Cambridge, Massachusetts 02138
(Received 26 December 1990)

- Carroll, Field, Jackiw, Phys. Rev. D 41 (1990)
- Antonucci, Ann. Rev. Astron. Astrophys. 31 (1993).
- Ivanov, Kovalev, Lister, Panin, Pushkarev, Savolainen, Troitsky, JCAP 02 (2019) 1811.10997
- Fujita, Tazaki, Toma, Phys. Rev. Lett. 122 (2019), 1811.03525
- Liu, Smoot, Zhao, Phys. Rev. D 101 (2020), 1901.10981.
- Caputo, Sberna, Frias, Blas, Pani, Shao, Yan, Phys. Rev. D 100 (2019).
- Chigusa, Moroi, Nakayama, Phys. Lett. B 803 (2020), 1911.09850.
- Chen, Shu, Xue, Yuan, Zhao, Phys. Rev. Lett. 124 (2020), 1905.02213
- …

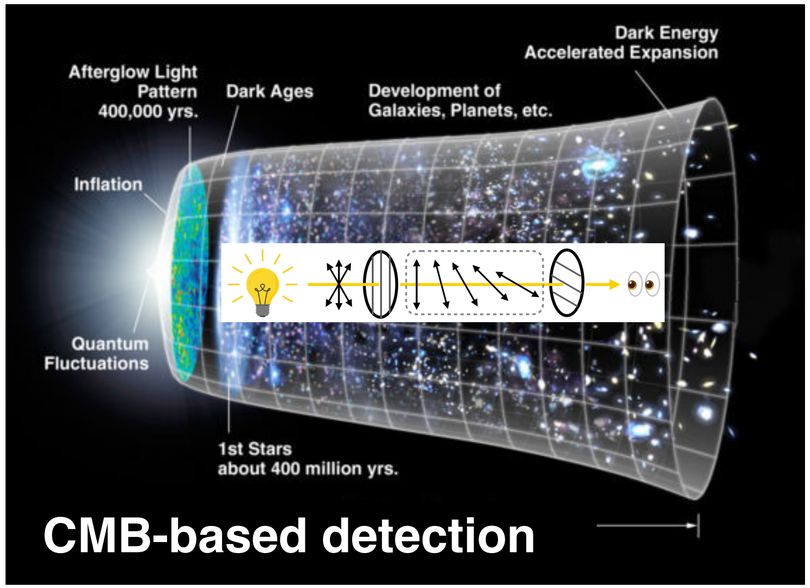

- Lue, Wang and Kamionkowski, Phys. Rev. Lett. 83 (1999)
- Feng, Li, Xia, Chen and Zhang, Phys. Rev. Lett. 96 (2006)
- Antonucci, Ann. Rev. Astron. Astrophys. 31 (1993).
- Planck Collaboration, A&A 596 (2016)
- …

A standard task for the CMB missions

Detecting ALDM with PPAs

Key points

- Being wave-like, ALDM induced cosmic birefringence is common and correlated among pulsars
- **PPAs** provide an excellent tool to study ***spatial correlations*** of the ALDM-induced signals, which are largely ignored in previous studies

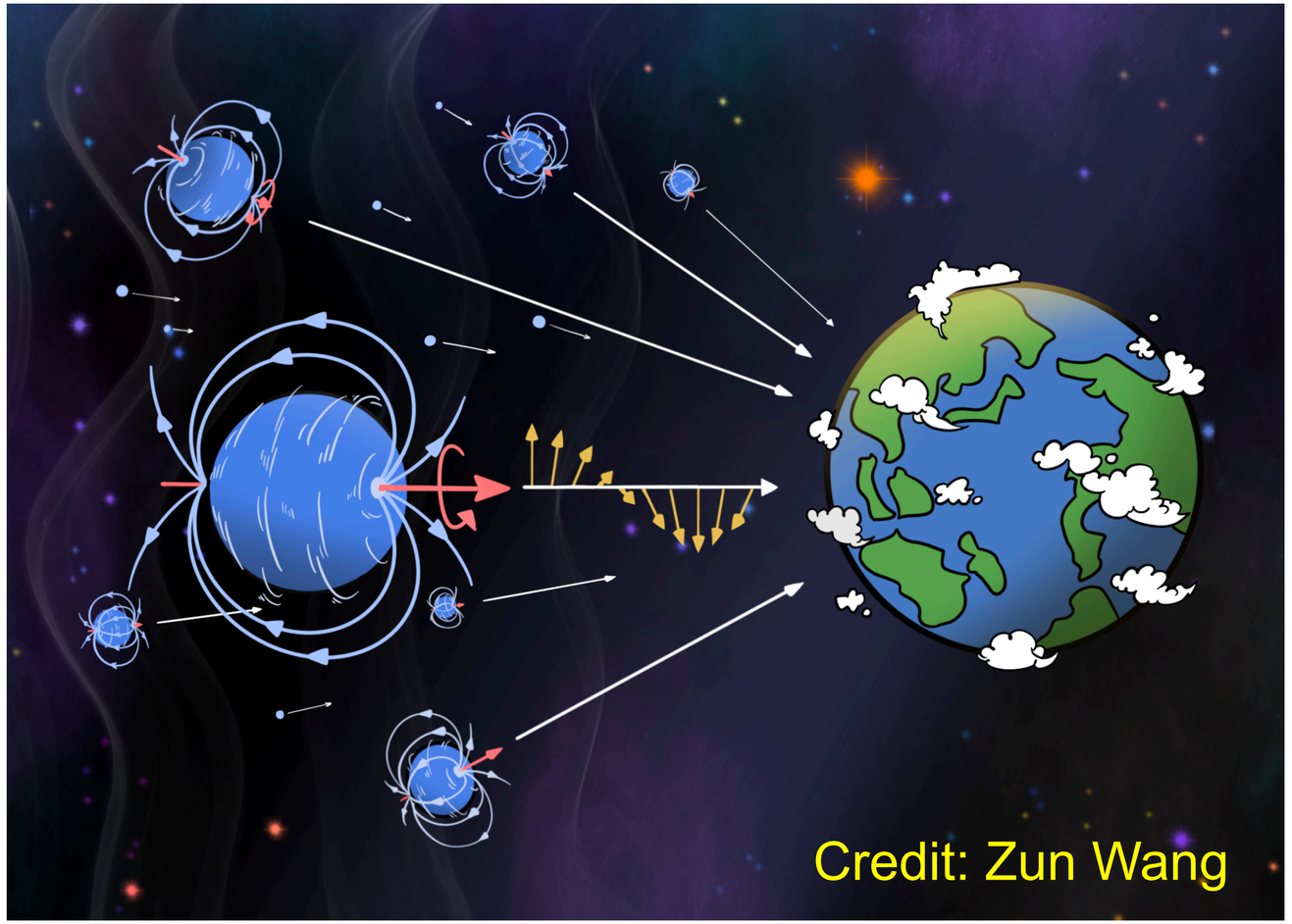

ALDM induced signal for PPAs

- PA rotation signal on PPAs characterized by the covariance matrix

$$C^a_{p,n;q,m} \approx \frac{g^2_{a\gamma\gamma}}{m_a^2}\left\{\rho_e \cos[m_a(t_{p,n}-t_{q,m})] + \sqrt{\rho_p\rho_q}\cos[m_a(t'_{p,n}-t'_{q,m})]\frac{\sin y_{pq}}{y_{pq}} + ...\right\} \quad y_{pq} = \Delta x_{pq}/l_c \quad l_c = 1/(m_a v_0)$$

(coherence length)

Comparison	SGWB	ALDM
Earth-term correlation	quadrupolar correlation	monopolar correlation (universal)
pulsar-term correlation	pulsar-terms suppressed in $L \gg 1/\omega$ limit; **spatial correlations rapidly degrade**	**spatial correlations degrade slower** ($L \gg l_c \gg 1/m_a$); encode DM density dep.; enhanced at galactic center

sin y/y encodes spatial correlation in the ALDM wave phase

- Current PTA (i.e. constant DM density for most pulsars): $C^a_{p,n;q,m} \approx S_a^2 \hat{C}^a_{p,n;q,m}$, $S_a = g_{a\gamma\gamma}\sqrt{\rho_e}/m_a$

$$\hat{C}^a_{p,n;q,m} \equiv \cos[m_a(t_{p,n}-t_{q,m})] + \cos[m_a(t'_{p,n}-t'_{q,m})]\mathrm{sinc}(y_{pq}) - \cos[m_a(t'_{p,n}-t_{q,m})]\mathrm{sinc}(y_{ep}) - \cos[m_a(t_{p,n}-t'_{q,m})]\mathrm{sinc}(y_{eq})$$

First Pulsar Polarization Array Limits on Ultralight Axion-like Dark Matter

Xiao Xue,[1,2] Shi Dai,[3] Hoang Nhan Luu,[4] Tao Liu,[5,*] Jing Ren,[6,7,†] Jing Shu,[8,7,9] Yue Zhao,[10] Andrew Zic,[3] N. D. Ramesh Bhat,[11] Zu-Cheng Chen,[12,13] Yi Feng,[14] George Hobbs,[3] Agastya Kapur,[3] Richard N. Manchester,[3] Rami Mandow,[15,3] Saurav Mishra,[16] Daniel J. Reardon,[16,17] Christopher J. Russell,[18] Ryan M. Shannon,[16,17] Shuangqiang Wang,[19,3] Lei Zhang,[20,16] Songbo Zhang,[21,3] and Xingjiang Zhu[22,23,24]

(PPTA Collaboration)

We conduct the first-ever Pulsar Polarization Array (PPA) analysis to detect the ultralight Axion-Like Dark Matter (ALDM), using the polarization data of 22 millisecond pulsars from the third data release of Parkes Pulsar Timing Array. As one of the major dark matter candidates, the ultralight ALDM exhibits a pronounced wave nature on astronomical scales and offers a promising solution to small-scale structure issues within local galaxies. While the linearly polarized pulsar light travels through the ALDM galactic halo, its position angle (PA) can be subject to an oscillation induced by the ALDM Chern-Simons coupling with electromagnetic field. The PPA is thus especially suited for the detection of the ultralight ALDM, by correlating polarization data across the arrayed pulsars. To accomplish this task, we develop a Bayesian framework dedicated to analyzing the time series of PA residuals of these pulsars. We find that the PPA provides the most stringent constraints on the ALDM Chern-Simons coupling so far for the mass range of $10^{-22} - 10^{-21}$ eV, pushing the upper limits to $10^{-13.5} - 10^{-12.2}$ GeV^{-1}. We finally demonstrate the crucial role of cross-correlation analysis in recognizing the nature of the derived limits.

submitted to journal (under review)

PA data construction and modeling

- Construction of time series of the observed PA residuals
  - PPTA DR3: 22 MSPs; T_{obs} ~18yr (2004-2022); up-to-date polarization calibration; high frequency band (3GHz)
  - Stokes parameters: $\{I_{n,k}, Q_{n,k}, U_{n,k}, V_{n,k}\}$ as a function of pulse phase (k) and observation epoch (n)
  - Observed PA residuals: standard PA profile subtracted and average over k for each observation

$$\Delta\mathrm{PA}_n^{\mathrm{obs}} = \frac{1}{2}\arg\sum_k \tilde{L}_k L_{n,k} e^{2i\mathrm{PA}_{n,k} - 2i\overline{\mathrm{PA}}_k}\,,\ \mathrm{PA}_{n,k} \equiv \frac{1}{2}\arctan\left(\frac{U_{n,k}}{Q_{n,k}}\right) \longrightarrow \langle\Delta\mathrm{PA}_n^{\mathrm{obs}}\rangle = \Delta\mathrm{PA}_n^{\mathrm{t}}$$ (unbiased estimator)

- Modeling of the observed PA residuals

$$\Delta\mathrm{PA}^{\mathrm{obs}} = \Delta\mathrm{PA}^{a} + \Delta\mathrm{PA}^{w} + \Delta\mathrm{PA}^{r} + \Delta\mathrm{PA}^{\mathrm{det}} + \Delta\mathrm{PA}^{\mathrm{iono}}$$

ALDM induced signal | white noise | red noise | deterministic residue | ionosphere corrections

Comprehensive expansion of the minimal noise model in literature

Ionospheric FR varies significantly over time (influence by solar activities), leading to unmodeled noise despite efforts for the ionospheric subtraction

Bayesian Analysis Framework

- Likelihood function: $\ln \mathcal{L} = -\frac{1}{2}\widetilde{\Delta \mathrm{PA}}^{T} \boldsymbol{C}^{-1} \widetilde{\Delta \mathrm{PA}} - \frac{1}{2}\ln|2\pi \boldsymbol{C}|\,.$

$$\widetilde{\Delta \mathrm{PA}} \equiv \Delta \mathrm{PA}^{\mathrm{obs}} - \Delta \mathrm{PA}^{\mathrm{ion}} - \Delta \mathrm{PA}^{\mathrm{det}} \qquad C = C^{w} + C^{r} + S_a^2 \hat{C}^{a}$$

Analytical marginalization of the deterministic residues (i.e. polynomial expansion)

$$\ln \mathscr{L}_m \propto \frac{1}{2}\left(\delta \mathrm{PA}^{c}\right)^{T} C_M^{-1}\, \delta \mathrm{PA}^{c} - \frac{1}{2}\ln|2\pi C_M| - \frac{1}{2}\delta \mathrm{PA}^{T} C^{-1}\, \delta \mathrm{PA} - \frac{1}{2}\ln|2\pi C|,$$

- Bayesian analysis with $\mathcal{L}_m(m_a, S_a, D_p, \theta_w, \theta_r)$. Find the 95% limit on S_a for each m_a
  - Maintain phase info: numerically marginalize pulsar distance D_p
  - Ensure consistency of noise modeling: comparing various noise models
  - Identify the nature of derived limits: comparing noise and various signal models, i.e.

    Cross-correlation: full-correlation v.s. auto-correlation ($\hat{C}^{a,\mathrm{auto}}_{p,n;q,m} = \hat{C}^{a}_{p,n;q,m}\delta_{pq}$)

Noise properties for individual pulsars

	Pulsar	Posterior				$\ln \mathrm{BF}^{\psi^{(0,1)}}_{\psi^{(0)}}$	$\psi^{(0,1,2)}_{\psi^{(0,1)}}$	$\psi^{(0,1,2)+w}_{\psi^{(0,1,2)}}$	$\psi^{(0,1,2)+w+r}_{\psi^{(0,1,2)+w}}$
		$\log_{10}\mathrm{EF}_p$	$\log_{10}\mathrm{EQ}_p/\mathrm{deg}$	$\log_{10} S^{\mathrm{r}}_p/\mathrm{deg}$	Γ_p				
1	J0437-4715	$0.69^{+0.03}_{-0.03}$	$-0.65^{+1.92}_{-5.07}$	$-0.92^{+1.88}_{-1.93}$	$-1.27^{+0.39}_{-0.49}$	399.4	326.7	12649.8	30.2
2	J0613-0200	$-0.19^{+0.05}_{-0.06}$	$0.72^{+1.81}_{-1.82}$	$-3.53^{+4.15}_{-3.68}$	$-1.74^{+2.69}_{-3.58}$	-2.5	1.1	12.5	-0.1
3	J0614-3329	$-0.18^{+0.06}_{-0.06}$	$-2.82^{+4.09}_{-4.11}$	$-3.26^{+3.78}_{-3.81}$	$-2.49^{+3.08}_{-3.65}$	-2.4	-0.8	2.4	-0.1
4	J0711-6830	$-0.09^{+0.03}_{-0.03}$	$0.51^{+1.81}_{-1.82}$	$-3.77^{+3.79}_{-3.48}$	$-1.92^{+2.69}_{-3.34}$	-3.0	-1.6	18.4	-0.4
5	J1017-7156	$0.03^{+0.03}_{-0.04}$	$-0.14^{+2.06}_{-5.66}$	$-3.76^{+3.98}_{-3.40}$	$-1.89^{+2.64}_{-3.60}$	-3.2	-2.6	5.2	-0.1
6	J1022+1001	$-0.05^{+0.04}_{-0.04}$	$-0.22^{+1.82}_{-1.83}$	$-1.62^{+2.59}_{-4.72}$	$-1.67^{+1.22}_{-2.84}$	-3.1	-3.2	22.8	0.8
7	J1024-0719	$-0.07^{+0.02}_{-0.03}$	$-3.02^{+4.22}_{-3.90}$	$-3.84^{+3.73}_{-3.34}$	$-2.27^{+2.89}_{-3.34}$	-3.2	-1.8	2.9	-0.1
8	J1045-4509	$-0.03^{+0.02}_{-0.02}$	$-3.22^{+4.02}_{-3.83}$	$-3.59^{+3.75}_{-3.57}$	$-2.21^{+2.72}_{-3.22}$	-3.5	-2.1	0.1	-0.1
9	J1125-6014	$-0.17^{+0.03}_{-0.03}$	$-2.74^{+4.00}_{-4.17}$	$-3.83^{+3.67}_{-3.38}$	$-2.03^{+2.77}_{-3.58}$	-3.6	-0.7	14.7	-0.2
10	J1545-4550	$-0.20^{+0.15}_{-0.16}$	$-0.21^{+1.86}_{-2.14}$	$-0.48^{+1.84}_{-1.84}$	$-0.05^{+0.61}_{-0.54}$	-2.6	-2.8	24.6	6.5
11	J1600-3053	$-0.08^{+0.05}_{-0.05}$	$-0.10^{+1.81}_{-1.82}$	$-4.12^{+3.61}_{-3.20}$	$-1.85^{+2.68}_{-3.34}$	-4.0	-3.4	17.9	-0.3
12	J1603-7202	$-0.07^{+0.02}_{-0.02}$	$-0.07^{+1.86}_{-1.96}$	$-3.60^{+4.72}_{-3.62}$	$-1.21^{+2.36}_{-3.60}$	-1.5	-2.3	4.5	-0.1
13	J1643-1224	$-0.04^{+0.02}_{-0.02}$	$-3.12^{+3.69}_{-3.89}$	$-2.75^{+3.91}_{-4.04}$	$-1.33^{+1.64}_{-3.34}$	-3.7	-2.5	-0.2	0.3
14	J1713+0747	$-0.10^{+0.06}_{-0.07}$	$-0.06^{+1.78}_{-1.78}$	$-2.13^{+2.56}_{-2.60}$	$-4.59^{+1.67}_{-1.71}$	200.6	115.6	924.7	6.6
15	J1730-2304	$-0.17^{+0.04}_{-0.04}$	$-0.15^{+1.79}_{-1.79}$	$-4.09^{+3.70}_{-3.22}$	$-1.72^{+2.46}_{-3.38}$	-5.1	-0.9	126.6	-0.1
16	J1744-1134	$0.01^{+0.03}_{-0.04}$	$-0.42^{+1.80}_{-1.81}$	$-1.87^{+2.76}_{-4.83}$	$-0.97^{+1.21}_{-2.61}$	-5.2	-4.1	227.8	0.4
17	J1824-2452	$-0.06^{+0.03}_{-0.03}$	$-3.15^{+3.89}_{-3.82}$	$-3.50^{+3.85}_{-3.62}$	$-2.12^{+2.51}_{-3.09}$	-4.1	-2.3	0.0	-0.0
18	J1857+0943	$-0.10^{+0.03}_{-0.03}$	$-2.04^{+3.73}_{-4.54}$	$-3.65^{+4.18}_{-3.52}$	$-1.62^{+2.48}_{-3.47}$	-1.9	-1.0	5.1	-0.1
19	J1909-3744	$-0.04^{+0.03}_{-0.03}$	$0.00^{+1.78}_{-1.78}$	$-0.25^{+1.82}_{-1.82}$	$-0.39^{+0.34}_{-0.34}$	49.4	27.9	3735.3	53.8
20	J1939+2134	$-0.20^{+0.06}_{-0.09}$	$0.08^{+1.84}_{-1.84}$	$-3.40^{+3.86}_{-3.72}$	$-2.00^{+2.64}_{-3.22}$	15.3	1.5	16.8	-0.3
21	J2145-0750	$-0.08^{+0.02}_{-0.02}$	$-2.69^{+4.07}_{-4.19}$	$-3.64^{+3.72}_{-3.43}$	$-2.56^{+2.86}_{-3.59}$	-3.2	0.7	5.2	0.1
22	J2241-5236	$-0.10^{+0.02}_{-0.02}$	$-3.14^{+3.83}_{-3.94}$	$-3.69^{+4.42}_{-3.45}$	$-1.44^{+2.45}_{-4.00}$	-3.3	-1.8	12.9	-0.0

DR3: after ionosphere subtraction

Noise models

- $\psi^{(0)}$ **(minimal model)**: minimal white noise + constant det.
- **(0,1), (0,1,2)**: det. expanded to 1, 2 order in *t*
- **+w (+r)**: + additional white (red) noise

Results

- **Most pulsars**: full model improves data fit compared to $\psi^{(0)}$; +w leads to more noticeable improv.
- **J0437, J1713 and J1909**: significant improvement with all three additional components

Individual pulsar limits on ALDM signal

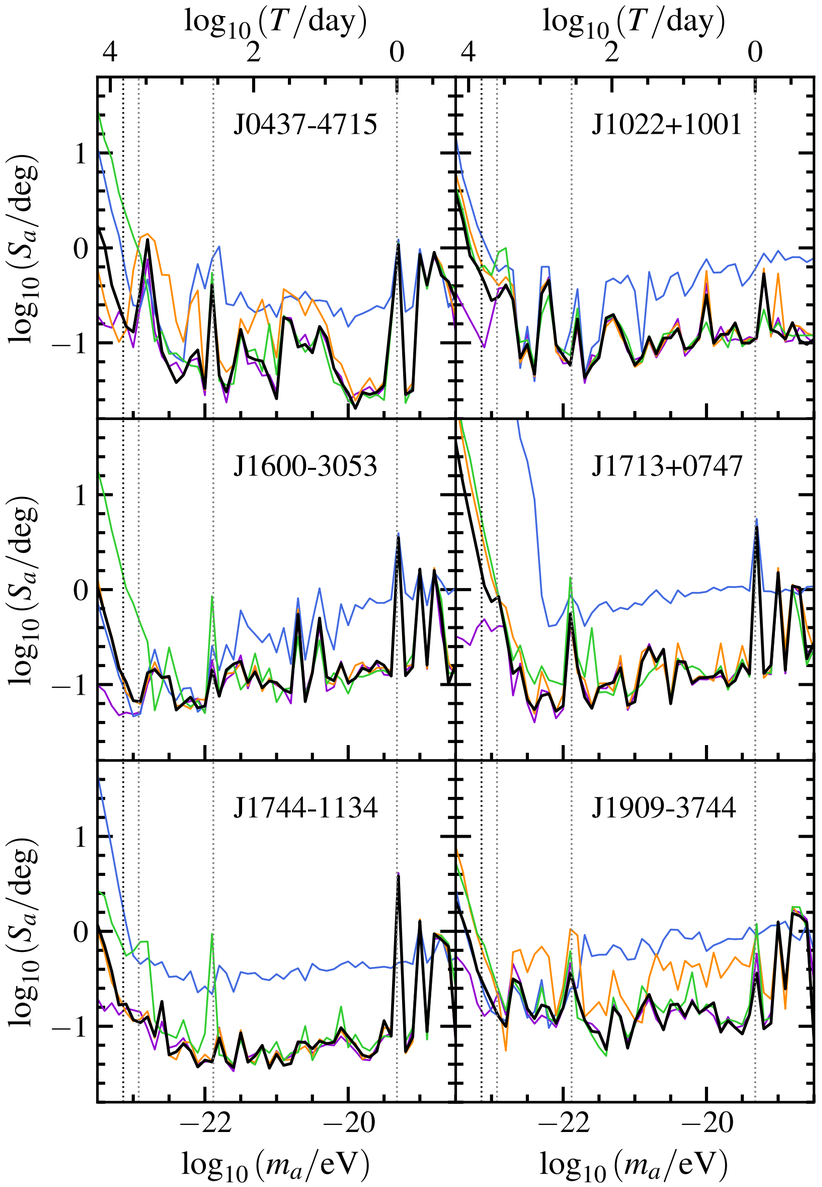

$$C^a_{p,n;q,m} \approx S_a^2 \hat{C}^a_{p,n;q,m}\,, \quad S_a \equiv \frac{g_{a\gamma\gamma}}{m_a}\sqrt{\rho_e}$$

- Black (**full noise model**); green (**w/o ionospheric corr**); blue (**w/o white noise**); orange (**w/o red noise**); purple (**w/o det**)
- **Ionospheric corrections:** ionFR model; efficient subtraction at T>1day, e.g. 1yr peak, excess at low frequency
- **White noise:** unmodeled ionospheric effects on short time; significant improvement of sensitivity for many pulsars
- **Red noises:** variation of ISM FR and unmodeled ionospheric effects over years; significant improvement at low frequency
- **$\Delta\mathrm{PA}^{\mathrm{det}}$ marginalization:** $S_a \sim$ const for $m_a > 1/T_{\mathrm{obs}}$, $S_a \sim (1/m_a)^3$ for $m_a < 1/T_{\mathrm{obs}}$
- **Sensitivity: $S_a < 0.1$deg or even lower** at $m_a > 1/T_{\mathrm{obs}}$ for J0437, J1744, J1022, J1600, …

- vertical lines: T_{obs}, solar cycle, 1yr, 1day

Upper limits on Chern-Simmons coupling

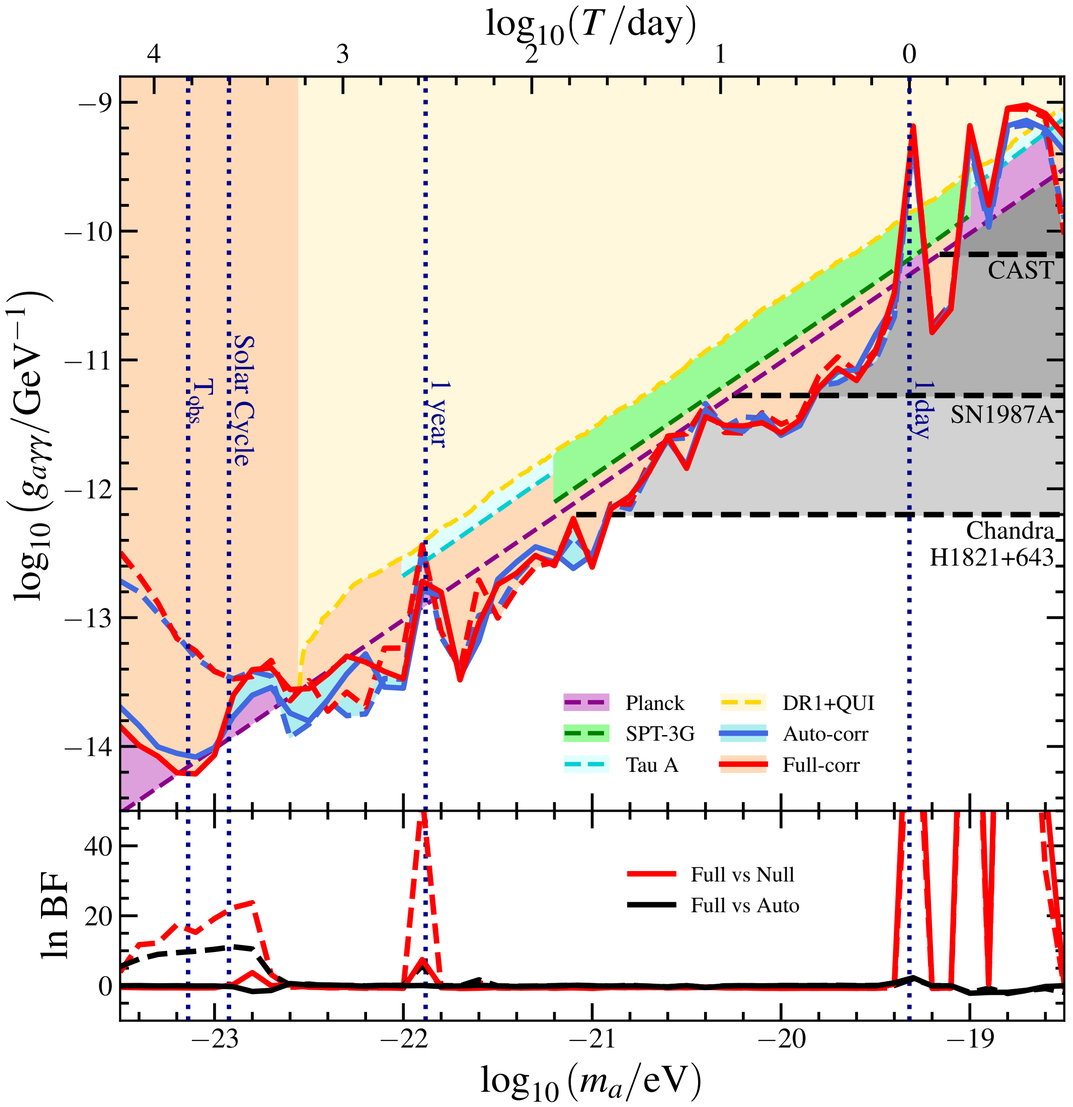

* solid/dash: with/without ionosphere

- Assuming observed local DM density: $\rho_e = 0.4\,\mathrm{GeV/cm^3}$
- Characteristic scaling: $g_{a\gamma\gamma} \propto m_a$ for $m_a > 1/T_{\mathrm{obs}}$; $g_{a\gamma\gamma} \propto m_a^{-2}$ for $m_a < 1/T_{\mathrm{obs}}$ ($T_{\mathrm{obs}} \sim 18\mathrm{yr}$)
- Model comparison:
  - **Full vs Null:** ionosphere subtractions help remove excess at T>1day
  - **Full vs Auto:** no excess at all m_a ⟶ shark peaks likely due to imperfect noise modeling

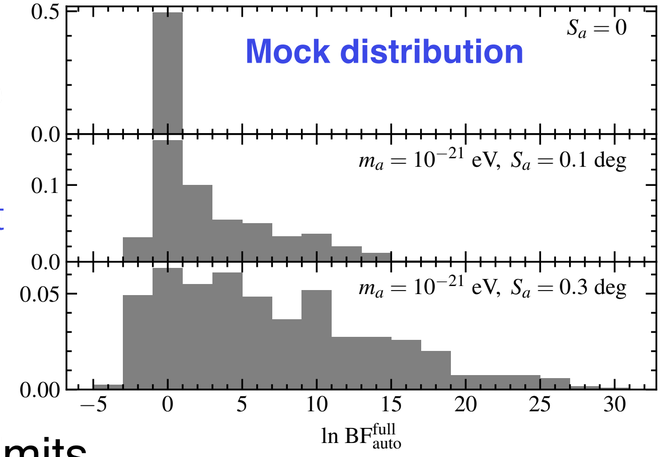

- Comparison with other limits
  - **ALP not DM** v.s. **ALP being DM:** the latter type provides stronger limits at lower frequency
  - Our PPA limits surpasses all other limits in mass range ~10^{-22}-10^{-21}eV; excellent sensitivity extends to ~10^{-23}eV

Gamma-ray PTAs

Science

REPORT | GRAVITATIONAL WAVES

A gamma-ray pulsar timing array constrains the nanohertz gravitational wave background

THE FERMI-LAT COLLABORATION Authors Info & Affiliations

SCIENCE • 7 Apr 2022 • Vol 376, Issue 6592 • pp. 521-523

DOI: 10.1126/science.abm3231

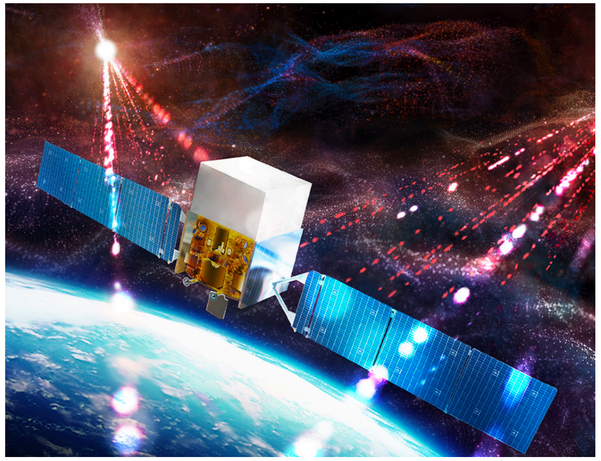

About 300 gamma-ray pulsars observed by Fermi-LAT (3rd catalog)

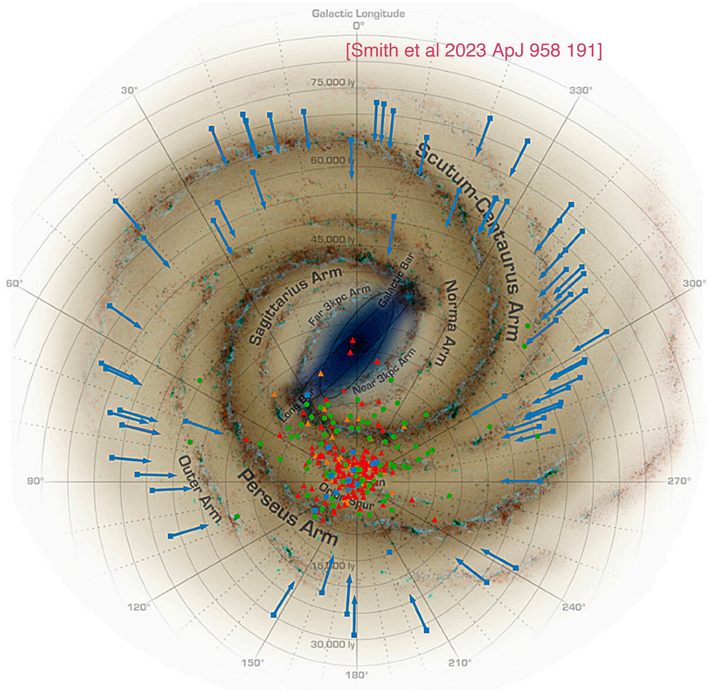

Credit: Photo By: Reid; M. J; et al.; Harvard-Smithsonian Center for Astrophysics

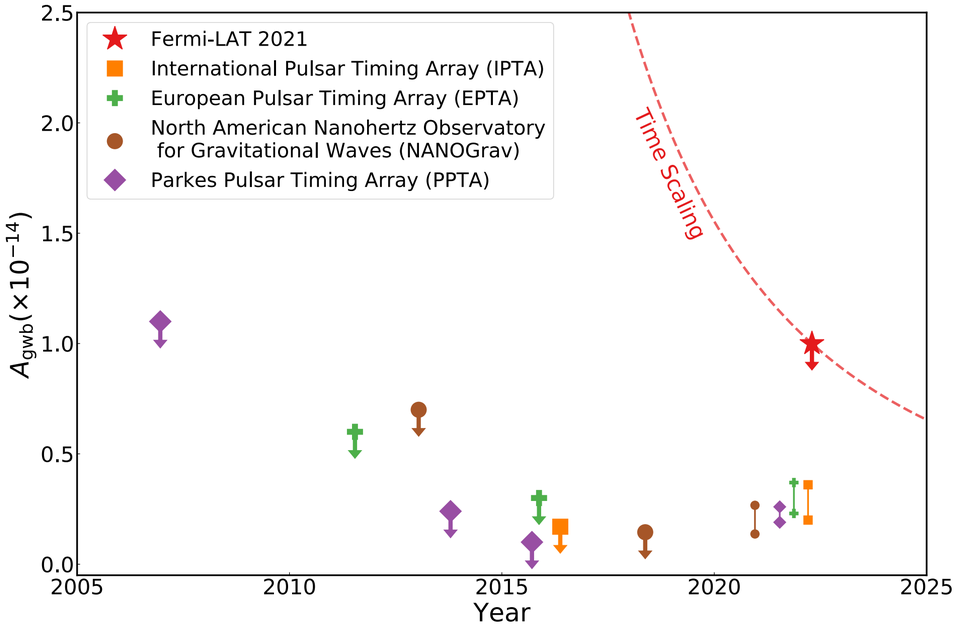

- "Con": limited statistics (small effective area), photo-by-photon method developed
- "Pro": Suppression of intrinsic red noise of dispersion measure variance
- An **independent check** for radio analysis

Gamma-ray PTAs for ULDM

TOA-based method

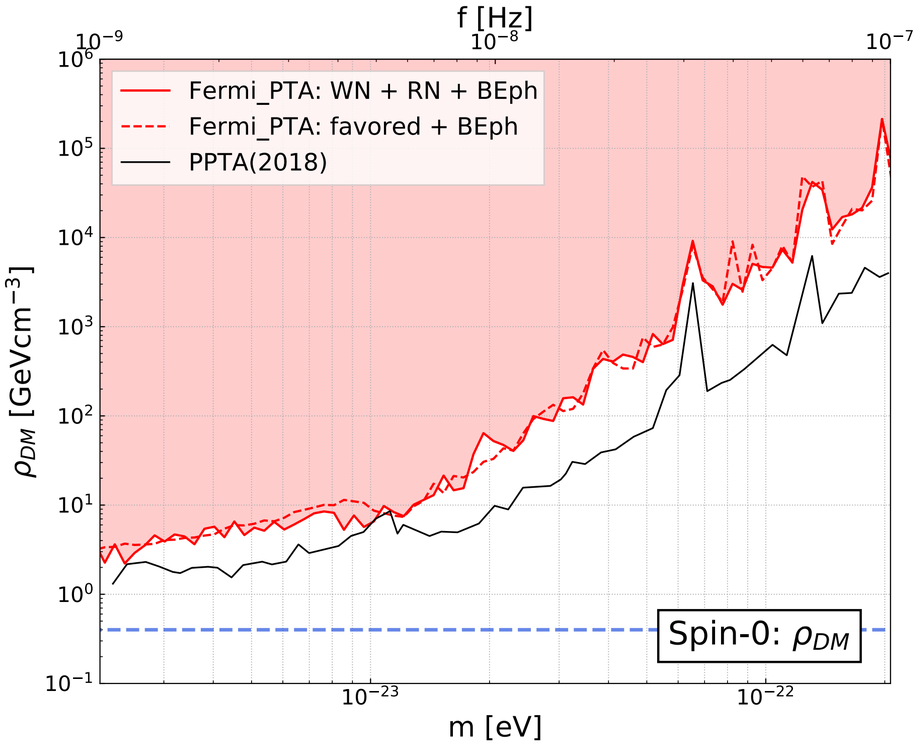

ULDM-induced signal being deterministic (DS)

[Xia, *et al.*, PRD 107 (2023)]

PBP-based method

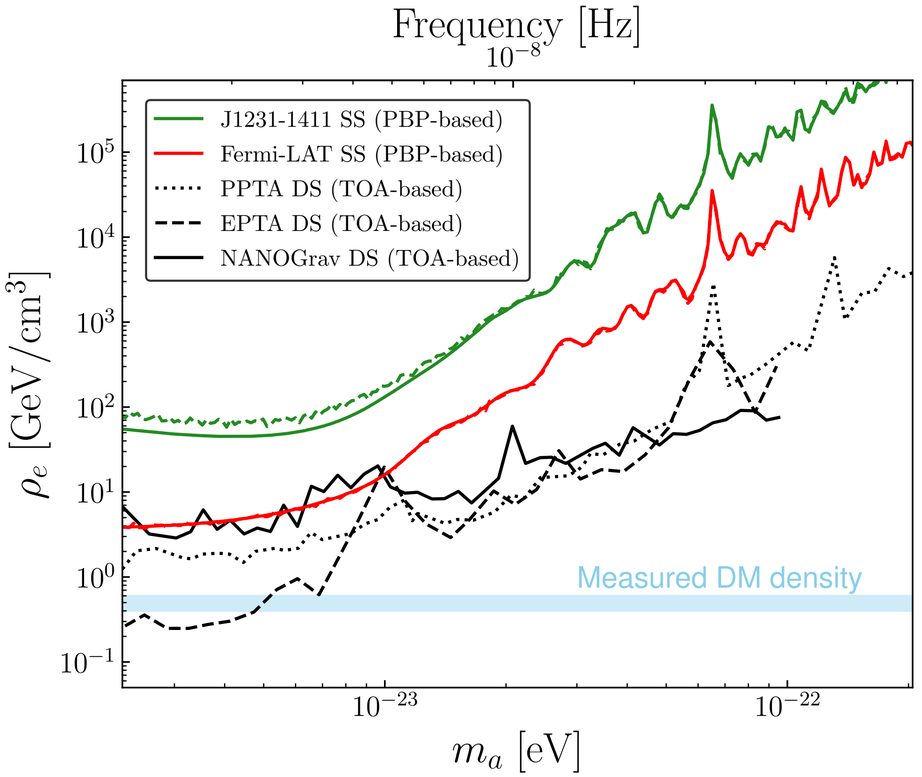

ULDM-induced signal being stochastic (SS)

[Luu, Liu, **JR**, *et al.*, Astrophys. J. Lett. 963 (2024)]

Future perspective

Frequency	Low-f band	High-f band
Timing	radio PTA 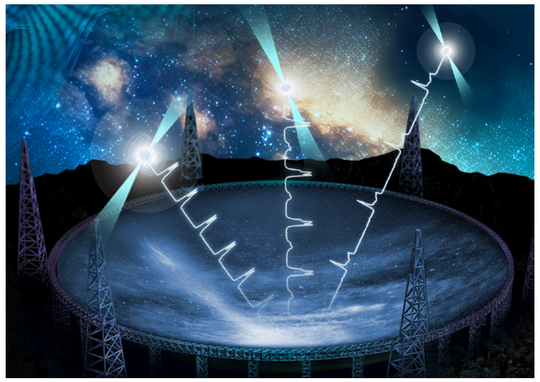	gamma -ray PTA 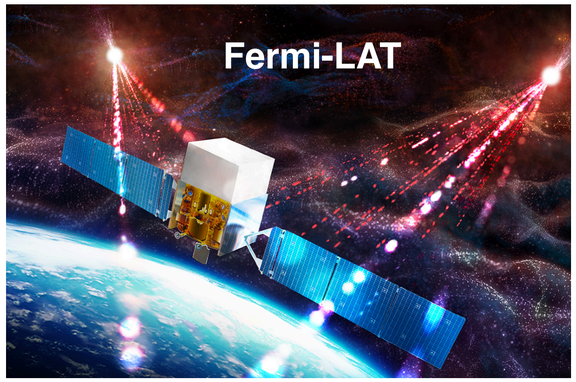
Polarization	radio PPA 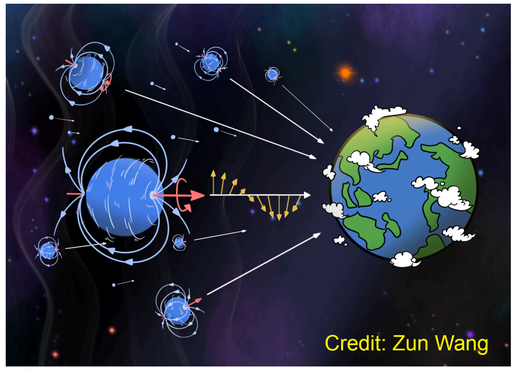	x-ray PPA (??)  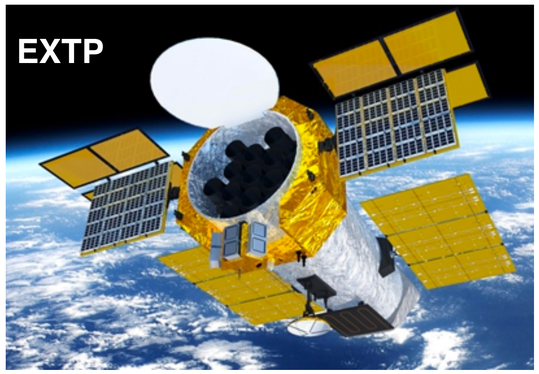

Summary and Outlook

- **PPAs:** a great tool to detect special correlations of ultralight ALDM
  - Develop a comprehensive data analysis framework for PPA detection of ultralight ALDM
  - Establish the first PPA limit on ALDM using PPTA DR3, providing the strongest limits on the Chern-Simons coupling in $m_a \sim 10^{-22}$ -10^{-21} eV
  - Highlight the crucial role of cross-correlation in recognizing the nature of derived limits

- **Outlook**
  - Real data analysis for PPAs: MeerKAT (regular pulsars); CPTA (excellent precison)
  - Cross-correlation of ALDM-induced signals on PPAs and PTAs
  - More physical targets for PPAs?
  - Synergize PPAs with other observations?

Thank You!